ADVANCED MATERIALS INTERFACES
www.advmatinterfaces.de

High Surface Area "3D Graphene Oxide" for Enhanced Sorption of Radionuclides

*Nicolas Boulanger, Anastasiia S. Kuzenkova, Artem Iakunkov, Andreas Nordenström, Anna Yu. Romanchuk, Alexander L. Trigub, Pavel V. Zasimov, Mariana Prodana, Marius Enachescu, Stephen Bauters, Lucia Amidani, Kristina O. Kvashnina, Stepan N. Kalmykov, and Alexandr V. Talyzin**

Here preparation of high surface area activated reduced graphene oxide (arGO) oxidized into a 3D analogue of defect-rich GO (dGO) is reported. Surface oxidation of arGO results in carbon to oxygen ratio C/O = 3.3, similar to the oxidation state of graphene oxide while preserving high BET surface area of about 880 $m^2 g^{-1}$. Analysis of surface oxidized arGO shows high abundance of oxygen functional groups which converts hydrophobic precursor into hydrophilic material. High surface area carbons provide the whole surface for oxidation without the need of intercalation and lattice expansion. Therefore, surface oxidation methods are sufficient to convert the materials into 3D architectures with chemical properties similar to graphene oxide. The "3D graphene oxide" shows high sorption capacity for U(VI) removal in an extraordinary broad interval of pH. Notably, the surface oxidized carbon material has a rigid 3D structure with micropores accessible for penetration of radionuclide ions. Therefore, the bulk "3D GO" can be used as a sorbent directly without dispersing, the step required for GO to make its surface area accessible for pollutants.

1. Introduction

Processing of radioactive wastes for long-term storage or permanent disposal is a challenging problem, which can be addressed using new materials. Many materials have been studied for the capture of radionuclides, including, for example, zeolites,[1] cement-based materials,[2] clays[3] and various kinds of carbon materials.[4] It is generally assumed that high surface area of material is an advantage for sorbent material.[5] However, most common high surface area carbons (graphene, graphitic carbons, and activated carbons) are not efficient for sorption of radionuclides due to the lack of suitable binding sites, such as oxygen containing functional groups.

Functionalization of carbon surface with various oxygen-containing groups has been demonstrated to increase sorption of radionuclides significantly. In particular, graphene oxide (GO) has been shown to provide a high sorption capacity for radionuclides and various heavy metals.[6]

GO is non-stoichiometric material with a somewhat uncertain molecular structure strongly depending on many factors, such as synthesis methods, ageing, and degree of oxidation.[7] The GO is functionalized mostly with epoxy and hydroxyl groups on the planar surface, while the edges of flakes are terminated mostly by carbonyls and carboxylic groups.[8] Moreover, the defects (holes and vacancies) are an essential part of the GO,[9] important for various applications.[10]

Our recent studies demonstrated that an increased number of defects and carboxylic groups in GO is correlated with the

N. Boulanger, A. Iakunkov, A. Nordenström, A. V. Talyzin
Department of Physics
Umeå University
Umeå S-90187, Sweden
E-mail: alexandr.talyzin@physics.umu.se

A. S. Kuzenkova, A. Y. Romanchuk, A. L. Trigub, P. V. Zasimov, S. N. Kalmykov
Department of Chemistry
Lomonosov Moscow State University
Leninskie Gory, Moscow 119991, Russia

The ORCID identification number(s) for the author(s) of this article can be found under https://doi.org/10.1002/admi.202200510.

DOI: 10.1002/admi.202200510

A. L. Trigub
National Research Centre "Kurchatov Institute"
Moscow, Russia

M. Prodana, M. Enachescu
Center for Surface Science and Nanotechnology
University Politehnica of Bucharest
Splaiul Independentei 313, Bucharest 060032, Romania

M. Enachescu
Academy of Romanian Scientists
Splaiul Independentei 54, Bucharest 050094, Romania

S. Bauters, L. Amidani, K. O. Kvashnina
Helmholtz Zentrum Dresden-Rossendorf (HZDR)
Institute of Resource Ecology
01314 Dresden, Germany

S. Bauters, L. Amidani, K. O. Kvashnina
The Rossendorf Beamline at ESRF
The European Synchrotron
CS40220, Grenoble Cedex 9 38043, France

improvement of sorption capacity for several radionuclides.[6b] This trend led us to the synthesis of extremely defect-rich modification of GO (dGO). The dGO has been prepared using Hummers oxidation of the defect-rich reduced graphene oxide (rGO) and demonstrated excellent sorption properties toward U(VI) with up to a 15-fold increase compared to standard GO.[11] The material was also demonstrated to exhibit specific selectivity in the sorption of organic pollutants.[12] The enhanced sorption of radionuclides has been correlated in these studies to interactions with carboxylic groups on the edges of flakes or holes and vacancy defects.[6b,11] Preferential interaction of metal cations with carboxylic groups is also in agreement with independent studies.[13] However, dGO requires relatively complex procedures for preparation, which increases costs. The synthesis might be challenging to scale up for real applications. Moreover, both GO and dGO need to be dispersed in water in order to make their high surface area accessible. The theoretical surface area of GO is about 2400 $m^2 g^{-1}$ (depending on oxidation degree) for a single-layered GO sheet.[14] However, the N_2 BET surface area of powder GO is negligibly small since the GO sheets are stacked in a multilayered structure, not allowing nitrogen to access the inter-layer space. The GO in aqueous dispersions prepared by sonication exhibit a smaller experimental surface area of 700–800 $m^2 g^{-1}$ determined by the sorption of various molecules.[5,15] Preparation of dispersions and removal of GO from solutions are technological steps, which complicate using these materials for practical applications.

An alternative approach to preparing carbon sorbents is the oxidation of common high surface area carbon materials. Several surface oxidation methods have been previously tested for carbon nanotubes,[16] activated carbons[17] and natural carbon materials like coals.[18] However, only very few of these materials have been tested for the sorption of radionuclides so far. Moreover, in some studies the surface area of tested carbon materials was relatively small, for example, <20 $m^2 g^{-1}$ for carbons produced by permanganate oxidation.[18] The most common method for surface oxidation of graphite or activated carbons is treatment by nitric acid.[19] However, several other chemical treatments aimed at surface oxidation have been studied for graphite and other carbon materials. These include, for example, direct oxidation by oxygen at elevated temperature[20] and chemical treatments using solutions of H_2O_2, NaOCl, $(NH_4)_2S_2O_8$, $AgNO_3$, H_2PtCl_6, etc.[21] It is likely that somewhat different types of functional groups will be attached to carbon material surface depending on the specific oxidation method but no systematic studies were so far performed for sorption of radionuclides by surface oxidized carbon materials.

Here we suggest that carbon materials with the type of surface functionalization similar to GO but easier in preparation and handling could be of interest for application as sorbents for removal of radionuclides. The sorbent materials for removing radionuclides were prepared using carbon material, which has a stable 3D structure with a high surface area modified by surface oxidation. Activated reduced graphene oxide (arGO), also named "activated graphene" in literature, is a high surface area material with up to 3000 $m^2 g^{-1}$ BET surface area, high micropore pore volume, and relatively low oxygen content.[22]

In this study, we report the preparation of surface oxidized arGO with high surface area (≈880 $m^2 g^{-1}$) as a new material with high sorption capacity for radionuclides in a broad pH range. The material demonstrates a porous 3D structure and does not require dispersion for sorption applications. Highly abundant surface functional groups similar to those found in GO make these materials extremely attractive as highly efficient sorbents for removing radionuclides from wastewaters. The oxidized arGO can be named "3D graphene oxide" due to the high degree of oxidation and sorption properties closely resembling the defect GO.

2. Results and Discussion

The main idea of this study is to produce carbon material with high surface area and high degree of surface oxidation. The surface oxidation of carbons with an extremely high surface area can be considered as an approach to the synthesis of highly oxidized carbon materials alternative to oxidation of graphite. Synthesis of graphene oxide includes two-step process: first intercalation and expansion of inter-layers (e.g., using H_2SO_4) in order to make all the surface area of individual graphene sheets accessible for oxidants and second is oxidation. High surface area carbons (activated graphene and activated carbons) provide the whole surface for oxidation without the need of intercalation and lattice expansion. Therefore, here we demonstrate that the surface oxidation methods are sufficient to convert the materials into GO-like 3D architectures.

The precursor arGO material was extensively characterized in our previous studies.[22a,b,23] It shows a relatively high BET surface area (2730 $m^2 g^{-1}$ for specific batch used here), microporous nature with a diameter of pores below 4 nm (**Figure 1**; Figures S1,S2, Supporting Information) and almost negligible amount of surface oxygen (C/O = 55). Several surface oxidation methods were tested in our study in order to achieve an oxidation degree similar to graphene oxide while keeping the BET surface area as high as possible.

Oxidation of arGO was first tested using the treatment by 10 M HNO_3 for different periods of time. The nitric acid treatment during 5 days resulted in efficient oxidation (C/O = 3.4) but also in a complete collapse of arGO porous structure providing material with BET SSA of only 25 $m^2 g^{-1}$. Therefore, the duration of acid treatment was reduced to 6 and 24 h. The samples will be named in following as nitric acid oxidized (NAO), NAO6h, and NAO24h, respectively (**Table 1**).

The treatment for 6 and 24 h resulted in the formation of moderately oxidized carbon materials (C/O = 8.2 and C/O = 6.0, respectively). This oxidation level is similar to the one typically observed in hydrophobic rGO (C/O ≈ 5–10) prepared by thermal or chemical reduction of GO.

The surface area of NAO decreased significantly compared to precursor arGO but remained relatively high (Table 1). Partial collapse of pore structure in nitric acid treated oxidized arGO is detected not only by the decrease of surface area but also evident in the analysis of pore size distribution (Figure S2, Supporting Information). The precursor arGO shows a relatively narrow pores size distribution with two peaks corresponding to pore diameters of ≈0.7–0.9 nm and ≈3–3.5 nm. The NAO materials demonstrate somewhat different pore size distribution with pores mostly below 1 nm in diameter. The change is also

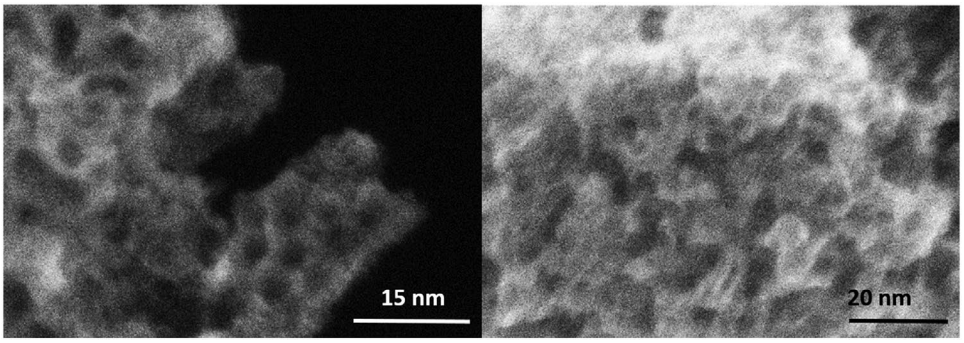

Figure 1. High resolution STEM images of arGO showing the porous structure of the material with most pores <4 nm in diameter.

reflected in pore volume which decreases from 2.30 $cm^3\ g^{-1}$ in precursor arGO to 1.05 and 0.39 $cm^3\ g^{-1}$ in NAO6h and NAO24h samples, respectively. (Figure S2, Supporting Information) The collapse of wider pores is responsible for the significant drop in SSA values. Some changes in the surface roughness are also evident in SEM images recorded from oxidized samples (Figure S3, Supporting Information).

The pore collapse and decrease of the surface area do not allow achieving higher oxidation degree using the HNO_3 oxidation method without the significant drop in surface area.

In contrast, ammonium persulfate oxidation (APO) of arGO resulted in a material preserving a significant surface area (880 $m^2\ g^{-1}$) and a high degree of oxidation. The decrease in surface area is mainly related to the collapse of pores with half pore width 10 to 20 Å abundant in rGO and nearly absent after oxidative treatments in all samples. The total pore volume of 0.46 $cm^3\ g^{-1}$ is found mostly in pores with diameter smaller than 3 nm. (Figure S2, Supporting Information). The smallest pores (<1 nm in diameter) are more stable against oxidation and, as earlier reported, also survive stronger mechanical treatment.[22b,24]

The C/O = 3.3 estimated for the APO sample using XPS is similar to the oxidation of carbon in graphene oxide. For example, this value is identical to oxidation achieved using one-step Brodie oxidation method (C/O = 3.4). The Brodie graphite oxide with that degree of oxidation exhibited swelling transitions and other properties typical for graphene oxide.[25] Following the definition of graphene oxide as an overall hydrophilic material, materials with C/O > 4 should be considered as rGO. These materials do not show swelling in water.[26] The "standard" graphene oxide has C/O in the range of ≈2–3.5 and shows swelling in polar solvents.[7f,8,27]

Table 1. BET Surface area, cumulative surface area calculated using QSDFT model, and C/O ratio of samples produced by surface oxidation of arGO using treatments by nitric acid (NAO) and ammonium persulfate (APO).

Sample	Oxidizing agent and reaction time	BET surface area [$m^2\ g^{-1}$]	DFT surface area [$m^2\ g^{-1}$]	C/O
arGO	none	2730	2260	55
NAO6h	10 M HNO_3 6 h	1810	1580	8.2
NAO24h	10 M HNO_3 24 h	830	920	6.0
APO	Ammonium persulfate 5 days	880	790	3.3

It can be concluded that the oxidation using ammonium persulfate is superior to nitric acid oxidation providing a higher oxidation degree while preserving relatively high surface area.

The nitric acid and ammonium persulfate methods are found to result in somewhat different types of surface oxidation, as revealed by XPS analysis. **Figure 2** shows the fitting of C1s spectra for precursor arGO, NAO6h, NAO24h, and APO samples. As expected, the main peak found in all four spectra is from not oxidized carbons (284.2–284.6 eV). Oxidized samples exhibit additional C1s components due to carbon atoms functionalized with several common oxygen groups. Remarkably, there is a major difference in the relative intensity of peaks typically assigned to epoxy and carboxylic groups. The strong 286.5 eV peak due to epoxy C—O groups is found in the C1s spectrum of APO sample while the samples oxidized using nitric acid demonstrate a stronger peak at 287.0–287.2 eV, which is typically assigned to carboxylic groups. The relative abundance of carbon atoms in carboxylic groups is somewhat larger in APO sample (15.1%) compared to NAO24h sample (12.0%).

In respect to the type of functionalization, the APO sample is more similar to graphene oxide (higher abundance of epoxy groups),[6b] while NAO samples resembles defect GO produced by oxidation of rGO.[11]

The similarity of the APO sample to GO is evident from an analysis of the thermal deoxygenation pathway revealed by TGA traces. The hydrophilic nature of the persulfate oxidized sample results in much stronger water sorption, which desorbs below 100 °C (about 15% weight loss). The main and rather steep weight loss step is observed in the TGA trace of APO at around 150–260 °C, similarly to the thermal de-oxygenation of typical Hummers GO (**Figure 3**).[27]

The weight loss of the NAO sample occurs almost linearly over a much broader temperature interval, indicating a more complex composition of material functionalized with a variety of oxygen groups (Figure S4, Supporting Information). The TGA trace of NAO shows more similarity to extremely defective dGO material analyzed in our earlier publications. It should be noted that TGA data cannot be used directly for the analysis of oxygen content in carbon materials since the thermal deoxygenation occurs with the formation of carbon oxide gases (CO_2 and CO).[28] That is also known to be the mechanism for thermal de-oxygenation in graphitic materials.[21] However comparing TGA traces on the relative scale clearly confirms stronger oxidation of the APO sample.

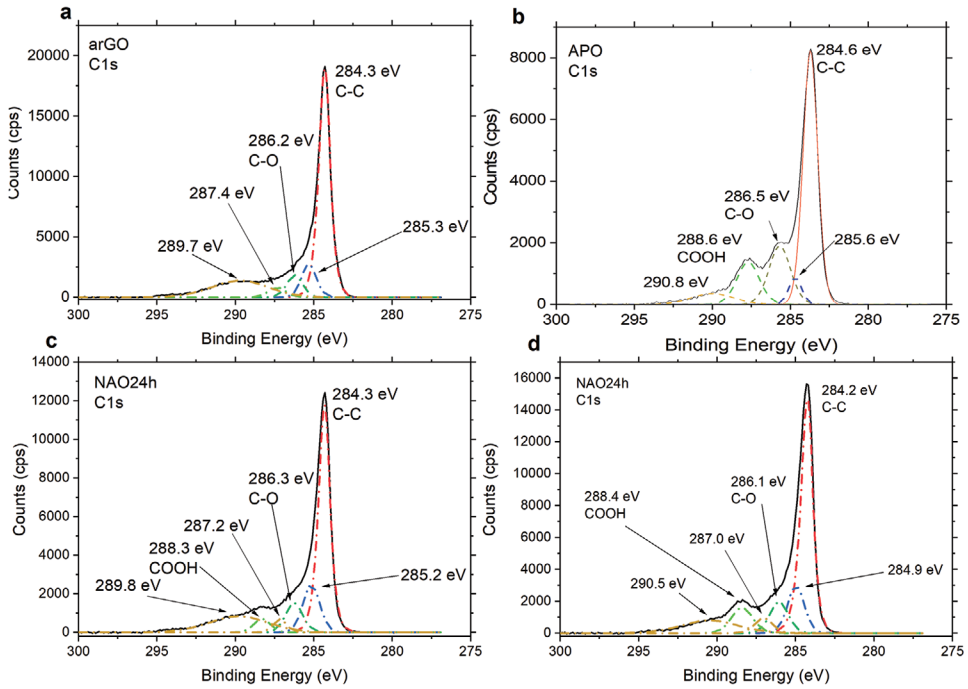

Figure 2. XPS C1s spectra of a) arGO, and arGO oxidized in b) ammonium persulfate, c) 10 M HNO_3 oxidized for 6 h, and d) 10 M HNO_3 oxidized for 24 h.

The hydrophilic nature of the APO sample was also confirmed by water sorption isotherm recorded using DVS (Figure S5, Supporting Information). The shape of isotherm and relatively high surface area (740 $m^2\ g^{-1}$) determined by water sorption are once again very similar to GO and sharply different compared to hydrophobic arGO (<10 $m^2\ g^{-1}$) The BET surface area determined by water sorption is only about 15% smaller compared to the BET surface area calculated using nitrogen isotherm. It can be concluded that most of the surface in APO material (at least 85%) is well oxidized.

Efficient oxidation of arGO was also confirmed using FTIR (**Figure 4**). The FTIR spectrum of the APO sample shows several strong peaks due to oxygen functionalization, most notable peaks at 1717 and 1205 cm^{-1} typically assigned to C=O and C—O groups. As expected from the lower oxidation of NAO24h, peaks from oxygen groups are much weaker in the FTIR spectrum of this sample. The APO spectrum also shows similarity to spectra of graphene oxide and even stronger similarity to spectra of dGO (Figure 4). The carbon framework of oxidized activated graphene is obviously very different from the 2D structure of graphene oxide, which results in the shift of C=O and C—O peak positions by 12 and 27 $cm^{-1,}$ respectively. However, the type of functionalization seems to be very similar since all the main features are present in both dGO and APO spectra (Figure S6, Supporting Information).

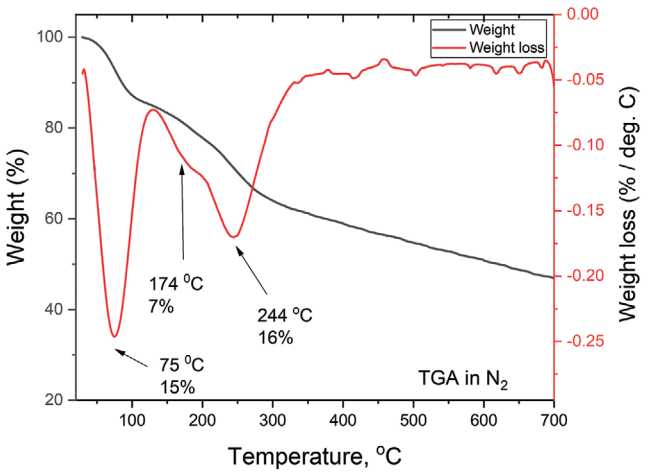

Figure 3. TGA traces recorded in nitrogen at 2 K min^{-1} for samples of arGO oxidized in ammonium persulfate.

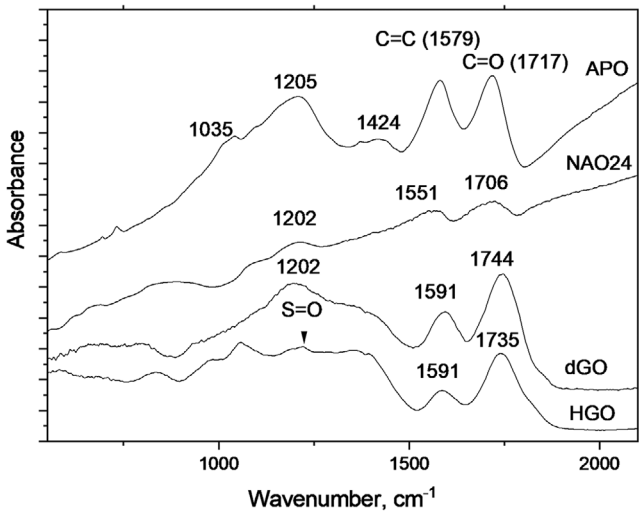

Figure 4. Spectrum of APO and NAO24 samples compared to spectra of standard Hummers graphene oxide (HGO) and defect-rich graphene oxide (dGO).[11]

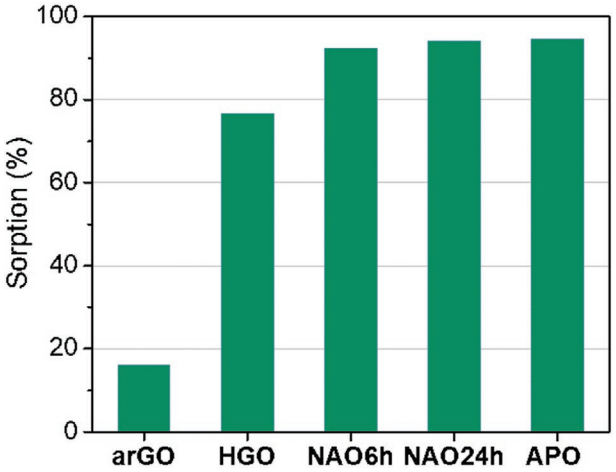

Figure 5. Sorption test: sorption of Am(III) in the presence of competing Al(III) ([solid] = 0.7 g L^{-1}, [Al (III)] = 1.3 g L^{-1}, pH = 3.5).

To evaluate the sorption properties of oxidized high surface area carbon materials, a rapid test was initially performed with Am(III) in the presence of Al(III) as a competing agent (**Figure 5**). The choice of competing agent is motivated by possibility to use high concentration of Al^{3+} in solution which allows achieving saturated sorption. We note also that mono- and divalent cations are not a high competitor to the sorption Am^{3+}.

The lowest sorption ability was found for non-oxidized arGO precursor material. As expected, a low amount of oxygen-containing functional groups is not favorable for the sorption of radionuclides. All oxidized materials demonstrate significantly higher sorption. The sorption capacity of oxidized carbons is also higher than for reference Hummers GO. Am(III) sorption tests showed that oxidized carbons have a high potential for application as radionuclides sorbent.

Therefore, a more detailed study was performed to evaluate the sorption properties of oxidized arGO to remove U(VI) from aqueous solutions. In particular, sorption isotherms and pH dependence of sorption were investigated.

The sorption isotherm allows us to estimate the sorption capacity of materials (**Figure 6**). As expected, U(VI) sorption

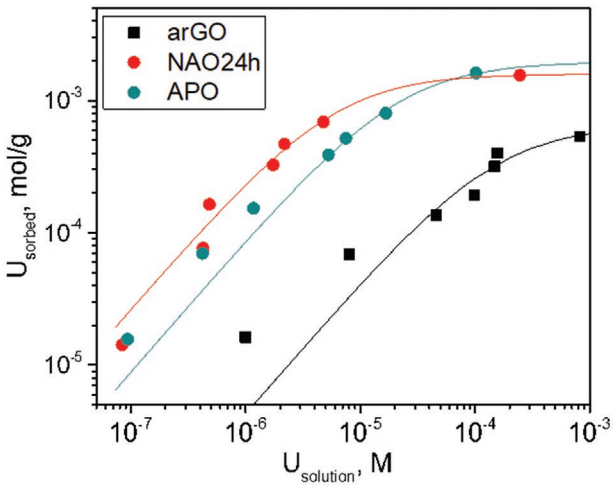

Figure 6. Sorption isotherms of U(VI) onto studied materials ([solid] = 0.5 g L^{-1}, pH = 5.1).

Table 2. Capacity for U(VI) sorption onto precursor arGO and two types of surface oxidized materials calculated by applying the Langmuir model at pH 5.1. Data for dGO are from ref. [11].

Sample	Maximum sorption capacity Q_{max} [μmol g^{-1}]
arGO	644 ± 78
NAO24h	1590 ± 38
APO	1950 ± 64
dGO	2250 ± 53

by arGO is dramatically lower compared to oxidized materials. All three oxidized arGO samples showed very similar sorption isotherms. Isotherms were fitted by the Langmuir model: $C_{sorb} = Q_{max}K_{La}C_{sol}/(1 + K_{La}C_{sol})$, where C_{sorb} is the equilibrium concentration of adsorbed radionuclides, C_{sol} is the equilibrium concentration of radionuclides in aqueous solution, Q_{max} is the maximum sorption capacity, and K_{La} is an adsorption coefficient. The calculated sorption capacities are presented in **Table 2**. The sorption capacity of oxidized materials toward U(VI) is very high. The highest sorption (1950 ± 64 μmol g^{-1}) was found for the persulfate oxidized arGO (APO sample). The APO sample is also the material with the strongest oxidation. The overall U(VI) sorption is slightly lower than sorption by previously reported extremely defective graphene oxide, dGO. However, APO has several advantages for sorption applications compared to dGO as discussed below.

Another essential characteristic of the sorbents is the pH region where they can work. **Figure 7** presents the pH edge of U(VI) onto APO compared with the natural sorbents, which are usually considered promising for removing uranium and some other radionuclides. APO shows very high U(VI) sorption in the wide pH range: from 2 to 11 similarly to dGO (Figure S8, Supporting Information). The sorption of U(VI) decreases dramatically with increasing pH over 7 because of the formation of the U(VI)-carbonate complexes in a solution that competes with the sorption. It is the unique feature of U(VI) sorption which needs to be addressed in advanced sorbents. Most of the known sorbents are not efficient for removing uranium at natural pH.

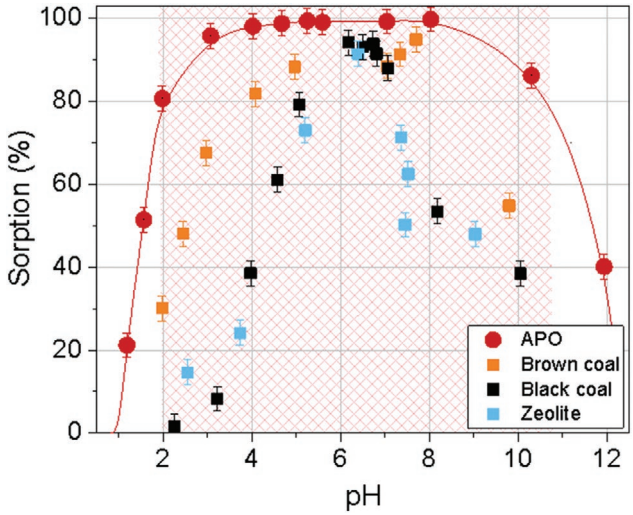

Figure 7. pH sorption edges for U(VI) onto APO in comparison with the published data on natural sorbents[29] ([U(VI)] = 2×10^{-7} M, [solid] = 0.5 g L^{-1}).

The oxidized high surface area carbon materials obtained in this work demonstrate high sorption even at pH higher than 8 because of the high amount of functional groups which serve as sorption sites for uranium. Natural sorbents cannot provide such an advantage.

It is clear that several types of oxygen functional groups are present on the surface of oxidized arGO. Therefore, we performed additional characterization of samples exposed to radionuclide solutions to study the sorption mechanism.

EXAFS spectra of U(VI) sorbed onto studied samples (**Figure 8**a) show that the local atomic environment of sorbed uranium is very similar in the case of APO and NAO24h samples. At the same time, these spectra are quite similar to U(VI) sorbed onto previously studied dGO samples. The parameters of the fit show good agreement among each other (Table S1, Supporting Information). In all these cases, the first peak of the Fourier transform at 1.3–1.4 Å is the U–O shell and can be addressed to two axial uranyl oxygen atoms in UO_2^{2+} cation. The next peak refers to equatorial oxygen atoms and latter subshell corresponds to U–C interactions. The EXAFS of U(VI) sorbed onto dGO, APO, and NAO24h indicate that the interaction occurs with carboxyl groups similar to the structures C4 (Figure 8; Figure S7, Supporting Information).

Rather different U(VI) local surrounding was observed in case of sorption onto precursor arGO sample. In this spectrum, third peak that correspond to U–C interaction is more pronounced. The number of oxygen functional groups in arGO is much lower and likely limited to very few kinds of functional groups. That is evidenced by a more ordered environment of uranium EXAFS spectra which leads to an increase in the intensity of the peaks. Moreover additional U–C distance appears in the fit at the distance 3.26 Å. This distance seems to appear when U binds not to carboxyl groups but to groups like C1 or C3 (Table S1, Figure S7, Supporting Information).

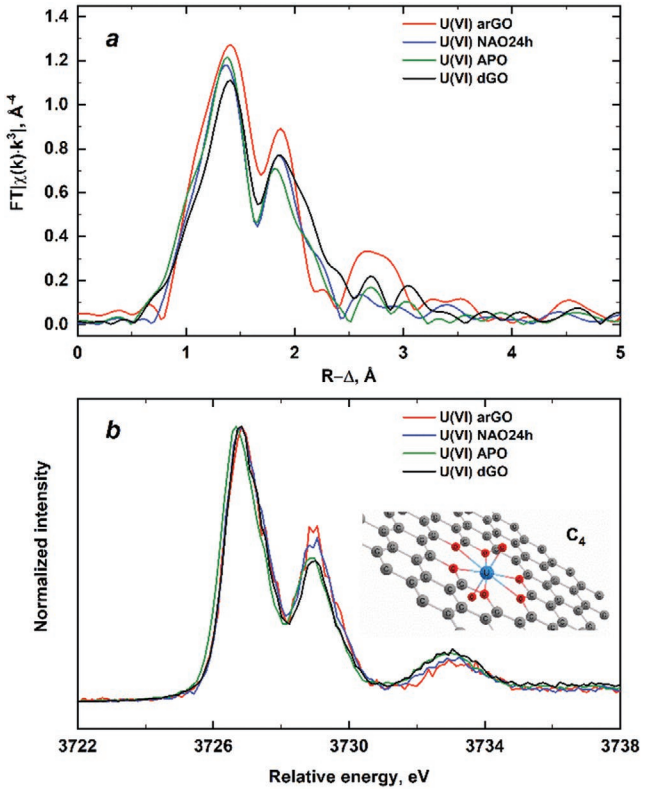

Figure 8. a) U L3 EXAFS spectra of U(VI) sorbed onto precursor arGO, NAO24h, APO, and dGO. b) U M4 HERFD-XANES spectra U(VI) for arGO, arGO oxidized in 10 M nitric acid for 1 day, and arGO oxidized in ammonium persulfate. The spectrum of defect graphene oxide (dGO) is provided for comparison. Inset shows C4 structure for U(VI).

The experimental U M_4 edge HERFD-XANES spectra[30] recorded after sorption experiments demonstrate three distinct features. (Figure 8b). The first intense peak corresponds to the transition to the 5fδ and 5fϕ U orbitals while two other features shifted from the first one by ≈2.1 and 6.2 eV, respectively, correspond to the transition to the 5fπ and 5fσ U orbitals.[31]

The height ratio for the second feature relative to the first is similar for U(VI) sorbed on dGO and APO samples (0.52) but increases in case of interaction with NAO24h (0.59) and in arGO (0.64) samples. In contrast, the relative intensity of the third peak decreases in the same sequence.

The HERFD-XANES spectra of oxidized samples are noticeably different compared to U(VI) sorption on precursor arGO. It can be concluded that the change in relative height of the main features of HERFD-XANES spectra correlates with the degree of oxidation.

Guided by the structural analysis of GO derived from the present EXAFS data (see the previous section), we performed FDMNES calculations of the U M4 edge HERFD-XANES for several structures similar to our earlier study for sorption of U(VI) in defects of GO.[6b,11] (Table S1, Figure S9, Supporting Information). Results (Figure S10, Supporting Information) indicate that the differences observed in experimental data are compatible with U(VI) adsorbed in holes for the more oxidized materials.

It can be concluded that modeling supports similarity between GO and APO materials with respect to mechanism of U(VI) sorption. The modeling results suggest that interaction of the radionuclides with GO and surface oxidized arGO occur on the small holes or vacancy defects.[6b,11]

The sorption capacity of surface oxidized arGO is likely related to overall number of carboxylic groups accessible on its surface. According to XPS data, the relative number of double bonded oxygen groups (C=O) is almost the same in APO and NAO24h samples (15.1% and 12.0% respectively). The surface area of APO is somewhat higher than in NAO24h (880 and 830 $m^2\ g^{-1}$, respectively) but the overall number of oxygen groups is almost twice higher (C/O = 3.3 in APO compared to C/O = 6 in NAO24h). Higher oxidation degree of APO material provides higher sorption of U(VI). As it is suggested by the spectroscopy data, certain geometrical configuration related to small holes in carbon sheets is most favorable for sorption but clearly not all carboxylic groups are arranged in the real material in that specific type of sites.

It needs to be emphasized that that surface oxidized materials presented in our study are extremely disordered. The precursor arGO is none-crystalline material without long range ordering. Oxidative treatment obviously makes the material even more defective as evident by partial collapse of pores and smaller surface area. Therefore, surface oxidation provides variety of oxygen functional groups and large variety of possible

sorption sites. The overall sorption is averaged over all possible sites.

The sorption capacity of APO samples is on the similar level as for previously reported dGO but with very clear advantages for practical applications. One of the main advantages of surface oxidized porous carbons presented in our study as compared to graphene oxides is easier synthesis. Hummers oxidation commonly is required to prepare graphene oxides and dGO starting from graphitic precursors. It is relatively complex procedure, which includes using concentrated acid, requires temperature control, slow adding permanganate in many steps, and known to be dangerous with certain risk of explosions. It is difficult to scale up Hummers oxidation for industrial production. In contrast, the surface oxidation by ammonia persulfate is rather simple one step procedure which can be applied to any high surface area porous carbon including not only arGO but also activated carbons. The oxidation method is easy to scale up for industrial production of materials in bulk amounts.

The 3D GO is also a material with rigid microporous structure, which is an advantage for the sorption applications compared to graphene oxides. The material can be applied to the sorption of contaminants from water by simple immersion and removal of powder. The surface area of GO is not accessible for sorption without dispersing this material to single sheets. The dispersions are typically produced using sonication or other strong mechanical treatments. The concentration of single-layered dispersions is not high (≈2–3 mg mL^{-1}) and large volumes of solvent are required for practical applications. Once the dispersion of single-layered GO sheets is exposed to contaminants, the sorption occurs and then the sheets need to be removed, for example, by filtration or centrifugation. It is particularly difficult to handle dGO material due to rather small particle size (tens of nm). As a result, dGO shows high sorption but difficult to use in standard filtration devices.

In contrast, "3D GO" which we report here is bulk porous powder material with micrometer size grains (Figure S3, Supporting Information). It can easily be used in standard filtration devices since the whole surface area of material is available for sorption without need for dispersing. Therefore, the powder 3D GO is compatible with standard filtration devices where bulk filler materials are used as sorbents to remove contaminations.

3. Conclusion

In summary, mild surface oxidation of "activated graphene" is demonstrated to result in the formation of high surface area carbon materials very similar to defect-rich graphene oxide but with 3D structure. The similarity in degree of oxidation, type of oxygen functionalization, hydrophilicity, and mechanism of radionuclide's sorption allows considering the new material as "3D graphene oxide" (3D GO).

The material demonstrates a porous 3D structure directly accessible for sorption of various contaminants. Highly abundant surface functional groups similar to those found in GO make these materials extremely attractive as highly efficient sorbents for removing radionuclides from wastewaters.

The material shows a relatively high surface area of about 880 m^2 g^{-1}, C/O = 3.3 and high capacity in sorption of U(VI) (1950 μmol g^{-1}). The sorption of radionuclides by surface oxidized materials is strongly enhanced compared to precursor arGO and standard graphene oxide. The 3D GO is easier to prepare but shows sorption capacity toward U(VI) comparable to dGO. It is also better compatible with standard filtration devices as a bulk powder material with surface area accessible for sorption of contaminants from solutions.

The high surface area of 3D GO is inherited from the precursor arGO but decreases significantly compared to the precursor due to oxidation-induced pore collapse. The collapse of pores was significantly less pronounced when ammonia persulfate was used as an oxidant instead of more common concentrated nitric acid.

Therefore, milder but similarly efficient surface oxidation methods might result in even better sorption capacity of 3D GO toward radionuclides. The hypothetical surface oxidized material similar to APO studied in our experiments but with surface area of ≈2700 m^2 g^{-1} (as in precursor material) will provide about three times higher number of oxygen functional groups per unit of volume. Therefore, the sorption capacity of the ideal hypothetical 3D GO could be expected to achieve an extraordinary value of ≈6000 μmol g^{-1}.

4. Experimental Section

Preparation of arGO: Graphite oxide powder was bought from Abalonyx (Product 1.8) and thermally exfoliated to produce rGO with maximal BET surface area following procedure tuned in the earlier studies.[32] According to this procedure, the graphite oxide powder (4 g) was placed inside of ≈1 L volume aluminum foil cylinder and rapidly inserted into a furnace at 230 °C for around 8 min. The GO powder explosively exfoliated during the rapid heating, thus producing powdered rGO. Providing sufficient volume for the explosion inside of the aluminium cylinder was essential in order to achieve maximal BET surface area.[32] To prepare activated graphene the rGO was subjected to KOH activation according to the procedure optimized in the earlier studies.[22a,b,32] The rGO powder was then mixed with potassium hydroxide in a 1:8 weight ratio in a 3:7 water:ethanol mixture and stirred overnight. The mixture was then dried overnight in a vacuum oven at 80 °C before being placed in a tube furnace under an argon flow. The furnace was heated up to 200 °C for 1 h in order to finish drying the material before being further heated to 850 °C and annealed at that temperature for 3 h before being slowly cooled down to room temperature. Afterward, the resulting material was stirred overnight in 1 L of a 10% acetic acid solution in water. It was finally rinsed using a vacuum filtration setup with a polytetrafluoroethylene (PTFE) membrane filter and dried overnight in a vacuum oven.

Surface Oxidation of arGO: The arGO powder was oxidized using two different methods: 1) using ammonium persulfate and 2) using nitric acid.

1) Typically 200 mg of arGO were placed in a container with an excess of saturated ammonium persulfate solution in DI water. The solution was left for stirring at room temperature for 5 days before being rinsed in a vacuum filtration setup with a PTFE membrane filter and dried in a vacuum oven.
2) For the oxidation in nitric acid, 500 mg of arGO powder was placed in a glass container in an oil bath at 80 °C. 10 mL of 10 M nitric acid was then added (50 mg arGO per mL of nitric acid), and the solution was left stirring in the now closed container for either 6 h or 1 day. The fumes from the acid were left escaping the container

in a tube and bubbled through a saturated KOH solution before being released in the fume hood. The solution was then rinsed with DI water in a vacuum filtration setup using a PTFE membrane filter before being dried in a vacuum oven.

Sorption Experiments: All sorption experiments were carried out in plastic vials with minimal retention by walls. The carbons suspensions were prepared by dissolving powders in water and mild sonication in a cavitation mode. It is important to note that mild sonication did not result in breakup of material's 3D porous structure. Aliquots of ^{241}Am and 1.3 g L^{-1} of Al^{3+} competitive cation were added to a 0.7 g L^{-1} solution in 0.1 M $NaClO_4$ for test sorption tests. The pH value was measured using a combined glass pH electrode (InLab Expert Pro, Mettler Toledo) with an ionomer (SevenEasy pH S20-K, Mettler Toledo) and was adjusted to 3.5 via the addition of small amounts of diluted $HClO_4$ or NaOH. After 24 h of equilibration the aliquot of the suspension were centrifuged at 40 000 g for 20 min (Allegra 64R, Beckman Coulter) to separate the solid phase from the solution. The sorption was calculated using the difference between the initial activity of the radionuclides and the activity measured in the solution after centrifugation. The activity of radionuclides was measured using liquid-scintillation spectroscopy (TriCarb 2700TR, Canberra Packard Ind., USA and Quantulus-1220, Perkin Elmer). The $^{232,233}U$ radionuclide was used in the pH-dependent sorption tests. A mixture of $^{232,233}U$ and natural uranium were utilized to create isotherms. In the case of pH dependence, experimental pH value was varied in the range of 1–12. The equilibration time was 24 h. In the isotherm experiment sorption systems were checked several days to maintain pH constant to the 5.1 ± 0.1. After several days of the equilibration on the constant pH conditions the sorption was measured using described above methods.

Statistical Analysis: The values of sorption capacity were represented as an average value ± standard deviation.

Supporting Information

Supporting Information is available from the Wiley Online Library or from the author.

Acknowledgements

A.V.T. acknowledges funding from the European Union's Horizon 2020 Research and Innovation Program under Grant agreement no. 785219 and no. 881603. A.V.T. acknowledges support from Swedish Research Council Grant (no. 2017-04173), acknowledge the Vibrational Spectroscopy Platform of Umeå University and A. Shchukarev for support with XPS test. L.A., S.B., and K.O.K. acknowledge help of J. Rothe, K. Dardenne, A. Beck, T. Prussman, and T. Vitova at the CAT-ACT beamline of KARA during the HERFD-XANES experiment at the U M_4 edge. The authors would like to thank S. Weiss from the HZDR safety group for his help in handling radioactive samples for the HERFD-XANES experiment. L.A, S.B., and K.O.K. acknowledge the support from the European Commission Council under ERC [Grant no. 759696]. A.S.K., A.Y.R., A.L.T, P.V.Z., and S.N.K. acknowledge support by the Russian Ministry of Science and Education under Grant no. 075-15-2021-1353. The work was also supported by Romanian Ministry of Research Innovation and Digitalization (M.E.), Romania, under ECSEL-JU POC 2014-2020 projects: OCEAN12 Contract no. 9/1.1.3H/20.01.2020 Code MySMIS 129948; PIn3S Contract no. 11/1.1.3H/03.04.2020 Code MySMIS 135127". Experimental studies were partially performed on the equipment acquired with the funding of M.V. Lomonosov Moscow State University Program of Development.

Conflict of Interest

The authors declare no conflict of interest.

Data Availability Statement

The data that support the findings of this study are available from the corresponding author upon reasonable request.

Keywords

graphene, graphene oxide, high surface area, radionuclides, sorption

Received: March 6, 2022
Revised: April 1, 2022
Published online: May 20, 2022

[1] a) E. H. Borai, R. Harjula, L. Malinen, A. Paajanen, *J. Hazard. Mater.* **2009**, *172*, 416; b) M. Pansini, *Miner. Deposita* **1996**, *31*, 563.
[2] a) L. De Windt, D. Pellegrini, J. van der Lee, *J. Contam. Hydrol.* **2004**, *68*, 165; b) K. F. Li, X. Y. Pang, *Cem. Concr. Res.* **2014**, *65*, 52.
[3] a) A. A. M. Abdel-Karim, A. A. Zaki, W. Elwan, M. R. El-Naggar, M. M. Gouda, *Appl. Clay Sci.* **2016**, *132*, 391; b) A. W. Miller, Y. F. Wang, *Environ. Sci. Technol.* **2012**, *46*, 1981; c) M. H. Bradbury, B. Baeyens, *Geochim. Cosmochim. Acta* **2005**, *69*, 875; d) C. B. Durrant, J. D. Begg, A. B. Kersting, M. Zavarin, *Sci. Total Environ.* **2018**, *610*, 511.
[4] a) M. R. Mahmoud, G. E. S. El-Deen, M. A. Soliman, *Ann. Nucl. Energy* **2014**, *72*, 134; b) Y. F. Wang, H. Z. Gao, R. Yeredla, H. F. Xu, M. Abrecht, *J. Colloid Interface Sci.* **2007**, *305*, 209; c) N. Savage, M. S. Diallo, *J. Nanopart. Res.* **2005**, *7*, 331; d) Y. A. Mackeyev, J. W. Marks, M. G. Rosenblum, L. J. Wilson, *J. Phys. Chem. B* **2005**, *109*, 5482.
[5] P. Montes-Navajas, N. G. Asenjo, R. Santamaria, R. Menendez, A. Corma, H. Garcia, *Langmuir* **2013**, *29*, 13443.
[6] a) A. Y. Romanchuk, A. S. Slesarev, S. N. Kalmykov, D. V. Kosynkin, J. M. Tour, *Phys. Chem. Chem. Phys.* **2013**, *15*, 2321; b) A. S. Kuzenkova, A. Y. Romanchuk, A. L. Trigub, K. I. Maslakov, A. V. Egorov, L. Amidani, C. Kittrell, K. O. Kvashnina, J. M. Tour, A. V. Talyzin, S. N. Kalmykov, *Carbon* **2020**, *158*, 291; c) A. Y. Romanchuk, A. S. Kuzenkova, A. S. Slesarev, J. M. Tour, S. N. Kalmykov, *Solvent Extr. Ion Exch.* **2016**, *34*, 594; d) L. Q. Tan, S. Wang, W. G. Du, T. Hu, *Chem. Eng. J.* **2016**, *292*, 92; e) C. L. Wang, Y. Li, C. L. Liu, *J. Radioanal. Nucl. Chem.* **2015**, *304*, 1017; f) Y. Xie, E. M. Helvenston, L. C. Shilller-Nickles, B. A. Powell, *Environ. Sci. Technol.* **2016**, *50*, 1821; g) Z. J. Li, F. Chen, L. Y. Yuan, Y. L. Liu, Y. L. Zhao, Z. F. Chai, W. Q. Shi, *Chem. Eng. J.* **2012**, *210*, 539; h) T. A. Duster, J. E. S. Szymanowski, J. B. Fein, *Environ. Sci. Technol.* **2017**, *51*, 8510; i) D. G. Gu, J. B. Fein, *Colloids Surf., A* **2015**, *481*, 319; j) Y. Xie, B. A. Powell, *ACS Appl. Mater. Interfaces* **2018**, *10*, 32086.
[7] a) H. P. Boehm, W. Scholz, *Z. Anorg. Allg. Chem.* **1965**, *335*, 74; b) S. You, S. M. Luzan, T. Szabo, A. V. Talyzin, *Carbon* **2013**, *52*, 171; c) A. M. Dimiev, L. B. Alemany, J. M. Tour, *ACS Nano* **2013**, *7*, 576; d) S. Kim, S. Zhou, Y. K. Hu, M. Acik, Y. J. Chabal, C. Berger, W. de Heer, A. Bongiorno, E. Riedo, *Nat. Mater.* **2012**, *11*, 544; e) A. Iakunkov, J. H. Sun, A. Rebrikova, M. Korobov, A. Klechikov, A. Vorobiev, N. Boulanger, A. V. Talyzin, *J. Mater. Chem. A* **2019**, *7*, 11331; f) T. Szabo, O. Berkesi, P. Forgo, K. Josepovits, Y. Sanakis, D. Petridis, I. Dekany, *Chem. Mater.* **2006**, *18*, 2740; g) K. Krishnamoorthy, M. Veerapandian, K. Yun, S. J. Kim, *Carbon* **2013**, *53*, 38.
[8] A. Lerf, H. Y. He, M. Forster, J. Klinowski, *J. Phys. Chem. B* **1998**, *102*, 4477.
[9] a) K. Erickson, R. Erni, Z. Lee, N. Alem, W. Gannett, A. Zettl, *Adv. Mater.* **2010**, *22*, 4467; b) Z. L. Liu, K. Norgaard, M. H. Overgaard, M. Ceccato, D. M. A. Mackenzie, N. Stenger, S. L. S. Stipp, T. Hassenkam, *Carbon* **2018**, *127*, 141.

[10] a) A. Gogoi, A. Koneru, K. A. Reddy, *Nanoscale Adv.* **2019**, *1*, 3023; b) P. Feicht, S. Eigler, *ChemNanoMat* **2018**, *4*, 244; c) P. Kaewmee, J. Manyam, P. Opaprakasit, G. T. T. Le, N. Chanlek, P. Sreearunothai, *RSC Adv.* **2017**, *7*, 38747.
[11] N. Boulanger, A. S. Kuzenkova, A. Iakunkov, A. Y. Romanchuk, A. L. Trigub, A. V. Egorov, S. Bauters, L. Amidani, M. Retegan, K. O. Kvashnina, S. N. Kalmykov, A. V. Talyzin, *ACS Appl. Mater. Interfaces* **2020**, *12*, 45122.
[12] S. Khaliha, T. D. Marforio, A. Kovtun, S. Mantovani, A. Bianchi, M. L. Navacchia, M. Zambianchi, L. Bocchi, N. Boulanger, A. Iakunkov, M. Calvaresi, A. V. Talyzin, V. Palermo, M. Melucci, *Flatchem* **2021**, *29*, 100283.
[13] a) R. R. Amirov, J. Shayimova, Z. Nasirova, A. Solodov, A. M. Dimiev, *Phys. Chem. Chem. Phys.* **2018**, *20*, 2320; b) R. R. Amirov, J. Shayimova, Z. Nasirova, A. M. Dimiev, *Carbon* **2017**, *116*, 356.
[14] J. H. Sun, F. Morales-Lara, A. Klechikov, A. V. Talyzin, I. A. Baburin, G. Seifert, F. Cardano, M. Baldrighi, M. Frasconi, S. Giordani, *Carbon* **2017**, *120*, 145.
[15] H. P. Boehm, A. Clauss, G. Fischer, C. Hofmann, *Proc. Fifth Conf. Carbon*, Pergamon Press, Heidelberg **1962**, p. 73.
[16] V. Datsyuk, M. Kalyva, K. Papagelis, J. Parthenios, D. Tasis, A. Siokou, I. Kallitsis, C. Galiotis, *Carbon* **2008**, *46*, 833.
[17] H. Guedidi, L. Reinert, J. M. Leveque, Y. Soneda, N. Bellakhal, L. Duclaux, *Carbon* **2013**, *54*, 432.
[18] A. Khannanov, V. V. Nekljudov, B. Gareev, A. Kiiamov, J. M. Tour, A. M. Dimiev, *Carbon* **2017**, *115*, 394.
[19] W. A. Abbasi, M. Streat, *Sep. Sci. Technol.* **1994**, *29*, 1217.
[20] H. P. Boehm, W. Heck, R. Sappok, E. Diehl, *Angew. Chem., Int. Ed.* **1964**, *3*, 669.
[21] H. P. Boehm, *Carbon* **2002**, *40*, 145.
[22] a) A. Klechikov, G. Mercier, T. Sharifi, I. A. Baburin, G. Seifert, A. V. Talyzin, *Chem. Commun.* **2015**, *51*, 15280; b) A. Iakunkov, V. Skrypnychuk, A. Nordenstrom, E. A. Shilayeva, M. Korobov, M. Prodana, M. Enachescu, S. H. Larsson, A. V. Talyzin, *Phys. Chem. Chem. Phys.* **2019**, *21*, 17901; c) Y. W. Zhu, S. Murali, M. D. Stoller, K. J. Ganesh, W. W. Cai, P. J. Ferreira, A. Pirkle, R. M. Wallace, K. A. Cychosz, M. Thommes, D. Su, E. A. Stach, R. S. Ruoff, *Science* **2011**, *332*, 1537; d) W. Y. Tsai, R. Y. Lin, S. Murali, L. L. Zhang, J. K. McDonough, R. S. Ruoff, P. L. Taberna, Y. Gogotsi, P. Simon, *Nano Energy* **2013**, *2*, 403.
[23] V. Skrypnychuk, N. Boulanger, A. Nordenstrom, A. Talyzin, *J. Phys. Chem. Lett.* **2020**, *11*, 3032.
[24] G. Moreno-Fernandez, N. Boulanger, A. Nordenstrom, A. Iakunkov, A. Talyzin, D. Carriazo, R. Mysyk, *Electrochim. Acta* **2021**, *370*, 137738.
[25] A. Klechikov, J. H. Sun, I. A. Baburin, G. Seifert, A. T. Rebrikova, N. V. Avramenko, M. V. Korobov, A. V. Talyzin, *Nanoscale* **2017**, *9*, 6929.
[26] U. Hofmann, A. Frenzel, E. Csalán, *Justus Liebigs Ann. Chem.* **1934**, *510*, 1.
[27] A. V. Talyzin, G. Mercier, A. Klechikov, M. Hedenstrom, D. Johnels, D. Wei, D. Cotton, A. Opitz, E. Moons, *Carbon* **2017**, *115*, 430.
[28] a) A. M. Rodriguez, P. V. Jimenez, *Thermochim. Acta* **1984**, *78*, 113; b) M. J. McAllister, J. L. Li, D. H. Adamson, H. C. Schniepp, A. A. Abdala, J. Liu, M. Herrera-Alonso, D. L. Milius, R. Car, R. K. Prud'homme, I. A. Aksay, *Chem. Mater.* **2007**, *19*, 4396.
[29] A. Semenkova, P. Belousov, A. Rzhevskaia, Y. Izosimova, K. Maslakov, I. Tolpeshta, A. Romanchuk, V. Krupskaya, *J. Radioanal. Nucl. Chem.* **2020**, *326*, 293.
[30] a) K. O. Kvashnina, S. M. Butorin, P. Martin, P. Glatzel, *Phys. Rev. Lett.* **2013**, *111*, 253002; b) K. O. Kvashnina, S. M. Butorin, *Chem. Commun.* **2022**, *58*, 327.
[31] L. Amidani, M. Retegan, A. Volkova, K. Popa, P. M. Martin, K. O. Kvashnina, *Inorg. Chem.* **2021**, *60*, 16286.
[32] A. G. Klechikov, G. Mercier, P. Merino, S. Blanco, C. Merino, A. V. Talyzin, *Micropor. Mesopor. Mater.* **2015**, *210*, 46.